able free water from SD. These might include the water potential gradient between juice and seed and the acidity of the juice. Even though previous work demonstrated no effect on germination of juice versus distilled water when applied as the germinating medium (15), the total soluble solids (TSS) and acids may be associated with in-fruit seed germination. Fruit produced in 1985-86 contained low TSS and acid (11) and in-fruit seed germination was highest. Low seed germination occurred in 1988 while brix and acid levels in the juice were high (11). Mobayen and Milthorpe (13) reported that citrus seed germination was delayed in high salt medium. If in-fruit seed germination in grapefruit depends on leaked juice from SD, it is probable that water movement from juice to seeds is more favorable when juice contains low TSS and acid because a greater water potential gradient occurs. Acids and TSS of juice from SD vesicles were lower than from normal vesicles (data not shown), however, no information is available about critical levels of water potential to allow water movement from juice to seed and subsequently seed germination. It is suggested that further studies should evaluate seasonal and grove changes in water potential gradient between juice components of healthy and disordered vesicles and the seeds and any influence this has on seed germination.

Literature Cited

1. Albrigo, L. G. and R. D. Carter. 1978. Structure of citrus fruits in relation to processing. Citrus Science and Technology. Vol. 1. S. Nagy, P. E. Shaw, and M. K. Veldhuis (eds.). p. 33-73. The AVI Publishing Co. Inc., Westport, CT.
2. Albrigo, L. G., K. Kawada, P. W. Hale, J. J. Smoot, and T. T. Hatton, Jr. 1980. Effect of harvest date and preharvest and postharvest treatments on Florida grapefruit condition in export to Japan. Proc. Fla. State Hort. Soc. 93:323-327.
3. Albrigo, L. G., M. A. Ismail, P. W. Hale, and T. T. Hatton, Jr. 1981. Shipment and storage of Florida grapefruit using unipack film barriers. Proc. Int. Soc Citriculture p. 714-717.
4. Awasthi, R. D. and J. P. Nauriyal. 1972. Studies on granulation in sweet orange (*Citrus sinensis* Osbeck). II. Effect of age, tree condition, tree aspect, fruit size, rootstock and tree variation on granulation. J. Res. 10(10:62-70.
5. Bartholomew, E. T., W. B. Sinclair, and F. M. Turrell. 1941. Granulation of 'Valencia' oranges. Calif. Univ. Agr. Expt. Sta. Bull. 647.
6. Burger, D. W. and W. P. Hackett. 1982. Influence of low temperature and gibberellic acid treatment on the germination of 'Valencia' orange seed. HortScience 17(5):801-803.
7. Chakrawar, V. R. and R. Singh. 1977. Studies on citrus granulation. I. Physical and quality aspects of granulation. Haryana J. Hort. Sci. 6:128-131.
8. Climatological Data, Annual Summary, Florida, 1985, 86, 87, 88. U.S. Dept. of Commerce, Environmental Data Service.
9. El-Zeftawi, B. M. 1978. Factors affecting granulation and quality of late-picked 'Valencia, oranges. J. Hort. Sci. 53:331-337.
10. Fahn, A., I. Shomer, and I. Ben-Gera. 1974. Occurrence and structure of epicuticular wax on the juice vesicles of citrus fruit. Ann. Bot. 38:869-872.
11. Florida Department of Agriculture & Consumer Services, Division of Fruit and Vegetable Inspection. 1986, 87, and 88. 1985-86, 1986-87, and 1987-88 season Annual Report, Winter Haven, Florida.
12. Mobayen, R. G. 1980. Germination of trifoliate orange in relation to fruit development, storage and drying. J. Hort. Sci. 55:285-289.
13. Mobayen, R. G. and F. L. Milthrope. 1978. Citrus seed germination as influenced by water potential and salinity. Proc. Int. Soc. Citriculture 2:247-249.
14. Noort, G. V. 1969. Dryness in navel fruit. Proc. 1st Int. Citrus Symp. 3:1333-1342.
15. Purvis, A. C. and L. G. Albrigo. 1984. Seasonal and temperature effects on seed germination in stored grapefruit. Proc. Fla. State Hort. Soc. 97:100-103.
16. Schneider, H. 1968. The anatomy of citrus. pp. 1-85. *In* The Citrus Industry. Vol. II. W. Reuther, L. D. Batchelor, and H. J. Webber (eds.). Univ. Calif. Div. Agr. Sci.

Proc. Fla. State Hort. Soc. 101:165-175. 1988.

AN APPROACH TO BETTER DESIGN OF PRESSURE-COOLED PRODUCE CONTAINERS

MICHAEL T. TALBOT
University of Florida, IFAS
Agricultural Engineering Department
Gainesville, Florida 32611

Additional index words. air cooling. airflow, heat transfer, modeling.

Abstract. **To determine a better method for design of the vent locations of pressure-cooled produce containers, a commercial finite element model was used to determine the pressure and velocity fields for air flow through a three-dimensional orange carton using porous media flow analysis. An existing heat transfer model incorporating the calculated pressure and velocity data was modified and used to calculate the cooling response for oranges packed in an experimental shipping container with six different vent arrangements. The calculated cooling response was compared to the experimental cooling response to evaluate the feasibility of porous media flow theory for the finite boundary condition of air flow through fresh produce packed in containers. Although several areas for improvement were noted, the porous media flow analysis was found to provide valuable information if variable porosity within the orange carton was considered.**

Florida Agricultural Experiment Stations Journal Series Number 9715.

Temperature is the most important environmental factor that influences the deterioration rate of harvested commodities. Thus improved cooling of fruits and vegetables before or during shipment, along with proper temperature maintenance throughout the marketing channels, has the potential of greatly reducing these losses.

Pressure- (forced-air) cooling is a popular precooling method developed by Guillou (7) extensively used on commodities which are highly perishable or susceptible to water-borne decay organisms. When applied for cooling of products in fiberboard containers, air is forced into and through the vented containers stacked and placed in the air circulation system. The air flows through the vents on the side of the containers exposed to the fan outlet, through the spaces between the products, out the side of the containers exposed to the fan outlet, and then back to the fan.

Although pressure cooling is a fairly rapid, efficient, and economical method of cooling of produce in containers, the containers must be designed carefully for proper operation of the system. Vent openings must be of proper size and in proper arrangements. Increasing the number of openings increases the uniformity of air movement at all points in the containers and therefore increases the uniformity of cooling with the containers.

In practice, how are the container vents currently selected? From the standpoint of the container manufactures, any location, number, and size of the vent holes can be produced to satisfy the customers desires. The major concern of the manufacturer is maintnance of the strength of the container, economy of material inputs, and customer satisfaction with an affordable container at a production profit. Cutting vents in the side panels of the containers can greatly reduce the stacking strength. The packinghouse personnel that procure the containers from the manufactures receive bids on containers with particular specifications of size, construction, vent patterns, shapes, and sizes, as well as, external printing. The distinctive and decorative packer or grower logo and other printed information common to a particular product may be of more importance than the venting specifications. Although some percentage of total vent openings may be specified as a rule or thumb or obtained from literature, the ultimate decision concerning container venting is more arbitrary than scientific.

What would be a better way to optimize the venting specifications of containers? The purest technique would be to conduct experimental evaluations of numerous combinations of vent patterns, sizes and shapes, with every combination of container size, product size, and packing configuration. The time and labor involved in such an effort are probably not feasible. However if a computer model were developed and verified with a limited number of experimental tests, this tool could be used to evaluate any number of venting and product packing combinations in a fraction of the time required for experimental analysis.

Talbot (13) summarized the considerable amount of published information on heat and mass transfer of fruits and vegetables and on various aspects of air cooling produce packed in shipping containers. No studies exist which predict the pressure and velocity fields for airflow through fruits or vegetables packed in shipping containers.

To understand and model airflow during pressure-cooling of fresh fruits and vegetables packed in fiberboard shipping containers, the pressure and velocity field characteristics within the container must be established. Both distributions are difficult to establish experimentally. There are many interrelated variables involved in air cooling of fruits and vegetables. These include thermal properties, physical properties, size, and shape of the product and temperature, flow rate and relative humidity of the cooling air. When cooling products in containers, additional variables of importance are container size, shape and wall thickness, venting and stacking arrangements, product packing configurations, and the direction of air flow.

Talbot (13) reviewed the historical evolution, diverse fields of application, and mathematical representation, of the theory of fluid flow through porous media. He also reported on numerous research studies of the cooling, heating, and drying of semi-infinite systems of bulk piled agricultural products such as fruits, grains, vegetables, nuts, and root crops using the theory of fluid flow through a porous media to determine the pressure and velocity fields.

The objectives of this study were to (1) determine the feasibility of the theory of flow through porous media analysis for finite boundary conditions of air flow through fresh fruits and vegetables packed in shipping containers, (2) use a commercial finite element model to predict air pressure and velocity distribution for air flow through fruits packed in fiberboard packing containers, and (3) compare the predicted cooling response data determined using the mathematical flow model in conjunction with an existing heat transfer model with the experimental cooling data.

Materials and Methods

The physical problem selected for modeling an individual carton packed with oranges, using porous media flow analysis, was an experimental box with dimensions similar to a commercial packing container used for oranges. The experimental box, with dimensions, is shown in Figure 1. The box was used in the evaluation of temperature response during cooling of the oranges and constructed to allow 10 possible air inlets or outlets for analysis of various air flow patterns through the box. The inlet/outlet holes were constructed by drilling holes in the sides of the box at the desired locations as indicated in Figure 1. Using threaded pipe flanges attached to the outside of the box, 1 inch (2.54 cm) inside diameter (i.d.) threaded pipes were installed so that the ends of the pipes were flush with the interior surface of the insulation.

A forced-air cooler designed specifically for research, with a capability of controlling all of the important variables relating to cooling biological materials, was used for this study (2). Air velocity, air temperature, relative humidity, container venting and product stacking arrangement were the variables that could be controlled. Temperature distribution within the individual product and within the product container, static pressure loss across the product container, and product moisture loss were among the parameters that could be measured.

Air entered the experimental carton through some combination of any three 1 inch (2.54 cm) inlet holes. The air passed through the product and exited through some combination of any five 1 inch outlet holes. The venting arrangements were obtained by the use of rubber stoppers which were large enough to seal the pipes at the inlet or exit vent. The vent openings which were not needed for a particular test were plugged. Table 1 presents the inlet and outlet combinations evaluated during this study.

The air flow rate leaving the carton was measured through the use of an "annubar" flow element installed in a 1 inch inside diameter pipe connected to the threaded pipe flanges attached to the outlet of the carton. When more than one outlet was used, a hot-wire anemometer was used to measure the relative flow leaving each hole. The flow rate was determined as a function of the difference between velocity pressure and static pressure. The pressure difference was measured with an electronic differential pressure manometer.

Twelve tests were conducted with an experimental orange carton packed with 18 kg of size 100 Valencia oranges using air flow rates ranging from 1.53×10^{-3} to

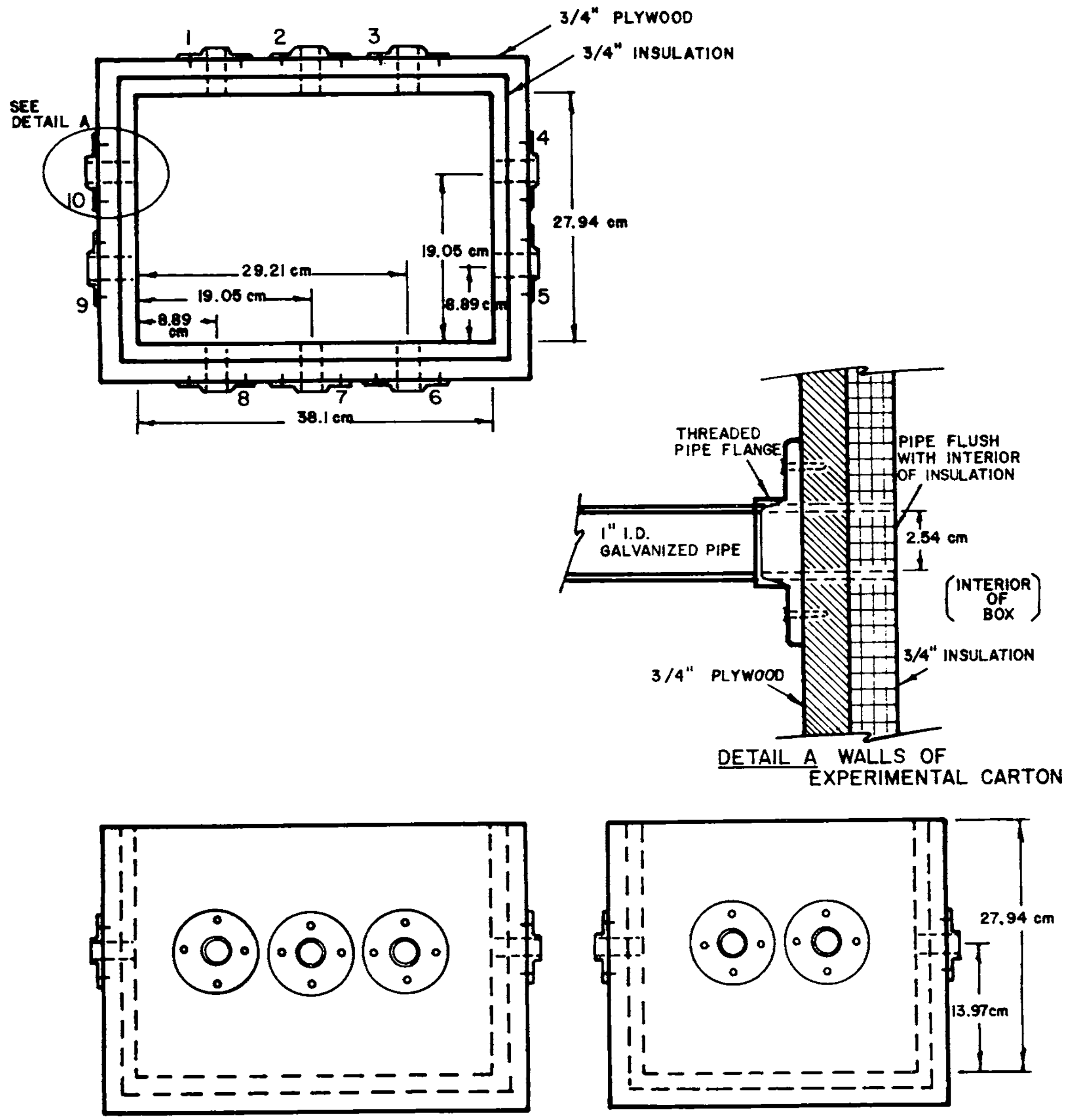

Fig. 1. The experimental orange carton.

2.06×10^{-2} m^3/s. These tests were conducted on 6 different venting arrangements with two flow rates for each. Considering the numbered vent locations shown in Figure 1, the flow patterns (boundary conditions) presented in Table 1, were evaluated.

Each cooling test was conducted using 88 sized fruit which were weighed and placed into the experimental orange carton in a face-centered cubic packing arrangement, which was the same configuration termed square-staggered by Chau et al. (3). This stacking pattern resulted in 5 horizontal layers of fruit, with 18 fruit in the bottom, middle and top layers and 17 fruit in the second and fourth layers. Thermocouples were placed at the center of 58 oranges and at the surface of 10 oranges. Ten thermocouples were also placed in the air spaces adjacent to the surface thermocouples to measure the air temperature within the orange carton. Other temperature measurement included the entering and leaving air temperatures. The thermocouples were constructed from 36-gauge, insulated copper-constantan wire. The location of the oranges in each layer of the thermocouples are shown in Figure 2.

Table 1. Boundary condition inlet/outlet vent locations and flow rates.

Boundary condition number	Inlet vents	Outlet vents	Balanced air flow rate, m^3/s per each inlet vent (1)	(2)
1	2	7	1.58 E-3	1.01 E-2
2	1, 3	6, 8	1.56 E-3	4.40 E-3
3	1, 2, 3	6, 7, 8	1.21 E-3	6.09 E-3
4	2	4, 7, 10	5.31 E-3	2.06 E-2
5	2	7, 10	4.72 E-3	1.33 E-2
6	1	6	1.53 E-3	5.46 E-3

Temperature was recorded on a microprocessor-controlled data acquisition system capable of receiving 80 thermocouple inputs. The product in the experimental orange carton was brought to a uniform temperature in the reheat section just prior to placement of the carton into the cooling chamber. The cooling air temperature was constant.

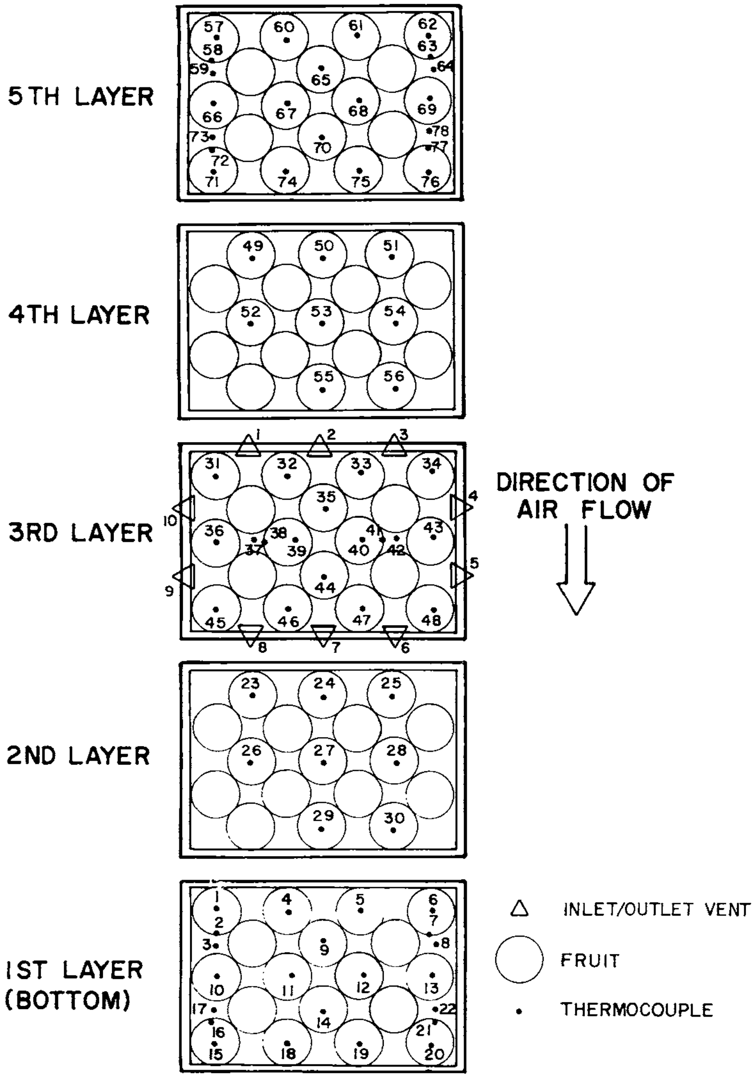

Fig. 2. Fruit and thermocouple locations in experimental orange carton.

After a literature review and temperature response data analysis, application of a 3-D finite element nonlinear porous media flow analysis for the problem under consideration was thought feasible. A general purpose commercial finite element analysis package, DeSalvo and Swanson (4), is available which contains an option that allows the modeling of nonlinear steady state fluid flow through a porous medium. This solution technique was studied and appeared to be applicable to the case at hand. A limited review was unable to identify other commercial solution packages which offered the needed analysis option and capabilities. In addition to evaluating the feasibility of the finite element porous media flow analysis, this study is also evaluating the feasibility of applying a commercial computer program.

The model description involves creating the desired geometry, selection(s) from the element library, specification of geometric (real) constants describing properties of elements, and identification of material properties (e.g., viscosity conductivity, and density).

The nonlinear porous media flow case involves the solution of the

(1) $[K]\{P\} = \{Q\}$

where

$[K]$ = the transmissivity matrix

$\{P\}$ = pressure vector (unknown)

$\{Q\}$ = mass flow rate vector

and the calculations of the pressure and mass flow distributions.

he momentum equation is simplified to

(2) $-(\text{grad } P) = \text{Reff } \bar{V}$

where

grad = gradient of a scalar function

P = pressure

$\bar{V}$ = seepage velocity vector

(3) $\text{Reff} = \mu/K + \beta\rho|\bar{V}|$

μ = gas viscosity

K = absolute permeability of porous medias

β = visco-inertial parameter

ρ = density.

Substituting Equation 2 into the continuity equation yields

(4) $\partial(k\partial P/\partial x)/\partial x + \partial(k\partial P/\partial y)/\partial y + \partial(k\partial P/\partial z)/\partial z = 0$

where $k = \rho/\text{Reff}$. Equation 4 is nonlinear because Reff is a function of velocity. The coefficients of permeability, k, are (kx, ky, kz) internally calculated for each coordinate direction as

(5) $k = K\rho/(\mu + K\beta\rho|\bar{V}|)$

Combining Equation 2 and 3 yields

(6) $-(\text{grad } P) = \mu\bar{V}/K + \beta\rho|\bar{V}|\,\bar{V}.$

In order to verify the calculated solutions of the commercial package, the solutions were used to solve porous media flow problems solved by other workers. The two-dimensional rectangular grain bin problem solved by Segerlind (11), one of the three-dimensional grain bin problems solved by Khompis et al. (8), and the pressure drop as a function of airflow for oranges in-bulk and in-cartons solved by Chau et al. (3), were modeled using the commercial package. Based on the results of this modeling, it was concluded that commercial package was an excellent analysis technique for investigating the pressure and velocity distributions in orange cartons.

The use of the porous media analysis to study the pressure and velocity distributions as air flows through a container of oranges presented several questions that were not significant problems for previous workers. A primary concern was the overall scale of the porous media used in this case. This scale was finite when ompared to the semi-infinite cases studied by others. Because of the small dimension of the packing container, boundary (wall) effects could be significant. The wall contact with the fruit or vegetable presented two possible difficulties. The drag caused as the air passes the wall was one consideration. The second concern, which has been reported by other workers (9, 10, 12) relates to the variance of the voidage or porosity adjacent to the walls when compared to the central portion of the porous media.

Other researchers have reported the significant pressure drops produced by the air inlets of packing containers. This point was another possible significant difficulty when comparing the pressure drop of the porous media (fruit or vegetable within the cartons) to that of the pressure drop across the inlet(s) and exit(s).

Another consideration in terms of fruits and vegetables was the compaction possible during packing and subsequent shrinkage with time due to physiological changes and moisture loss. The porosity may change, for example, if the product becomes more compact due to shrinkage or handling. The porosity next to the inside top of the carton could increase allowing more air to pass through this area.

The modeling of the experimental work of Chau et al. (3) was expanded to model an individual carton packed with oranges. The physical problem selected for solution was the experimental box shown in Figure 1.

An 8 node 3-D isoparametric thermal solid element, which allowed modeling of nonlinear steady-state flow through a porous media, was used. The node and element locations are shown in Figure 3. The model consisted of 1815 nodes and 1400 elements. The nodes adjacent to the walls of the experimental box were placed 1.5 inch (3.81 cm) from the walls in order to account for the locations of the vent openings. The remaining interior nodes were placed every 1 inch.

The boundary conditions for the air flow rates were obtained from the experimental temperature response study of size 100 square staggered packed oranges and the flow patterns and flow rates are shown in Table 1. The boundary conditions were specified at the nodal locations corresponding to the inlets and outlets vent locations, which were point sources. The no-flow or impermeable boundary condition $\partial P/\partial n = 0$, was automatically enforced on the boundary when no pressure values were specified.

The input coefficients needed to use the commercial finite element program are indicated in Equation 3. The gas viscosity and the density for air were taken from standard data tables. The absolute permeability of the porous media and the visco-inertial parameter are derived from

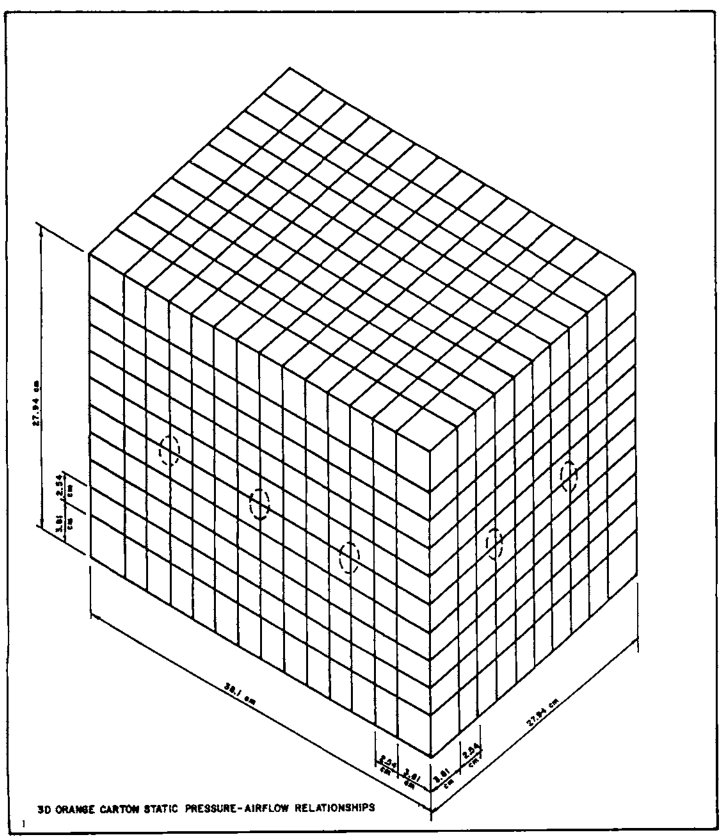

Fig. 3. The node and element locations used to model a three-dimensional orange carton.

experimental results. Chau et al. (3) presented a variation of the Ergun equation as

(7) $\Delta P/h = K_1 \mu V_s(1-\epsilon)^2/D_p^2 \epsilon^3 g_c + K_2 \rho V_s^2 (1-\epsilon)D_p\epsilon^3 g_c$

where

ΔP = pressure loss or head
h = the length of the flow path
V_s = the superficial velocity
ϵ = porosity = void volume/total volume
D_p = mean diameter of particles of the porous material
K_1, K_2 = experimentally determined Ergun product coefficients
g_c = Newton's Law gravitational constant

and the rest of the symbols are as previously defined.

Comparing Equation 7 and Equations 2 and 3, the absolute permeability of the porous media, K and the visco-inertial parameter, β, needed for the model input can be equated as

(8) $1/K = K_1 [(1-\epsilon)^2/D_p^2 \epsilon^3]$

and

(9) $\beta = K_2 [(1-\epsilon)/D_p\epsilon^3]$.

Chau et al. (3) detrmined K_1 and K_2 by fitting the experimental data and reported all the parameters required to solve Equations 8 and 9 for bulk packed oranges. For size 100 oranges arranged in a square staggered stacking pattern the following values were reported: $D_p = 0.0735$ m; $\epsilon = 0.405$; $K_1 = 1566$; and $K_2 = 2.22$.

In addition, the air viscosity and density were assumed not to vary significantly during the cooling process, and the values for these properties were obtained for an average test temperature of 50°F (10°C) $\mu = 1.762 \times 10^{-5}$ kg/m-sec; and $\rho = 1.24$ kg/m³.

Before solving Equations 8 and 9, the important topic of variable porosity must be considered. A comparison of the temperature response calculated by commercial program using the constant porosity and derived input parameters specified above with the corresponding experimental temperature response, produced poor agreement. Predicted temperatures were warmer in regions adjacent to the walls of the container and slightly cooler in the central portion of the container away from the walls. The concern for the variation of the voidage or porosity adjacent to the walls was expressed above and concluded to be the major factor resulting in the poor fit of the experimental temperature response. These preliminary comparisons are not presented, rather the input parameters were adjusted to account for the anticipated variable porosity as described below.

The distance of penetration from the wall of the variable porosity for oranges packed in a three-dimensional orange carton is a subject requiring additional research. Ridgway and Tarbuck (10) reported that the variation in porosity of large random beds existed to about 5 sphere diameters from the wall. Pillai (9) indicated the porosity variation could penetrate up to three particle diameters from the wall for two-dimensional randomly packed beds, but concluded that assuming a constant porosity byond one particle diameter would result in an error of less that 10%. For the current study, calculation of the porosity adjacent to the walls of the carton was possible using basic geometric relationships. However, the calculations beyond the first set of elements were complex due to the overlapping of the oranges in the three-dimensional stacking pattern. Therefore, the variable porosity was calculated within the regions occupied by the finite elements adjacent to all 6 interior walls of the experimental orange carton. Due to the size of the elements adjacent to the wall the variable porosity was calculated in a region one-half the orange diameter from each wall.

The procedure for calculating the porosity adjacent to the walls was accomplished by first assuming the oranges were perfect spheres. The volume of the oranges or portion of an orange lying within the elements and the volume of the elements adjacent to the wall were calculated. The porosity was defined in Equation 7 as the ratio of the void volume to total volume. The void volume was calculated by subtracting the volume of the oranges from the volume of the elements. The total volume was the volume of the elements adjacent to the walls.

The porosity for the elements was calculated using a more accurate technique (numerical integration) than employed by Talbot (3). Talbot indicated the porosity of the remaining 800 elements in the central portion of the carton remained equal to the constant porosity reported by Chau et al. (3). However, since the overall of void volume did not change, the porosity of the central portion should have been reduced to correspond to the increase in the porosity of the elements adjacent to the walls. The porosity of the different element types is shown in Table 2.

The commercial program has the capability of assigning individual material properties (β, K, etc.) to each individual element. Therefore, the Equations 8 and 9 were solved based on the porosity for each of the selected groups of elements considered and using the values of D_p, K_1, and K_2 specified above. The results of these calculation for β and K are shown in Table 2. The model was used to solve the 12 orange carton air flow boundary conditions presented in Table 1.

The porous media analysis output provided the total velocity (magnitude of the velocity vector) and the 3 components of the velocity vector at the centroid of each element (Figure 4), in addition to the element volume and pressure gradient. To obtain the necessary data for the heat transfer model, the output was reorganized using the Post-Processor and 3 Fortran programs (13).

The objective of the current study was not to devote a considerable amount of time in developing a specific heat transfer model before the feasibility of the porous media flow approach was assessed. Further it was considered essential that a validated heat transfer model be applied so as to concentrate the evaluation on the flow model results rather than attempting to simultaneously validate both the porous media flow analysis and a heat transfer analysis.

The literature contains many citations of heat and mass transfer models. However, the approach of this study was to use the one-dimensional explicit finite difference numerical model for individual fruit using heat transfer equations for a homogeneous sphere without heat sources reported by Baird and Gaffney (1), without major changes and to modify the numerical model to predict temperature distribution within bulk loads of products (bed model) also reported by Baird and Gaffney in such a way to treat each of the model generated elements as a bed. Each three-dimensional element interacted with surrounding elements.

Table 2. Summary of variable porosity and input data.

Element location	Number of elements	Porosity, ϵ	K	β
Center	800	0.319	2.3588E-7	641.1
Corners	8	0.440	9.1536E-7	200.9
Edges	112	0.578	3.7406E-6	66.0
4 Surfaces, 27.94 x 38.1 cm	384	0.522	2.0978E-6	102.7
2 Surfaces, 27.94 x 27.94 cm	128	0.529	2.2487E-6	97.2

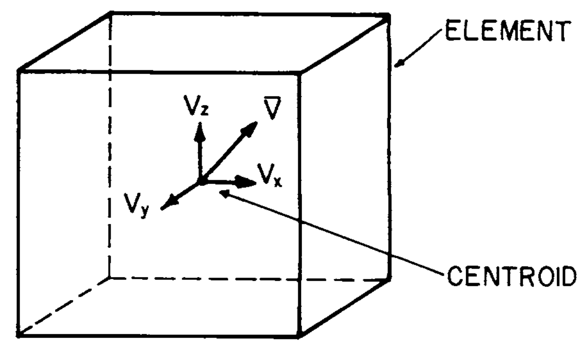

VELOCITY VECTOR AND THREE COMPONENTS

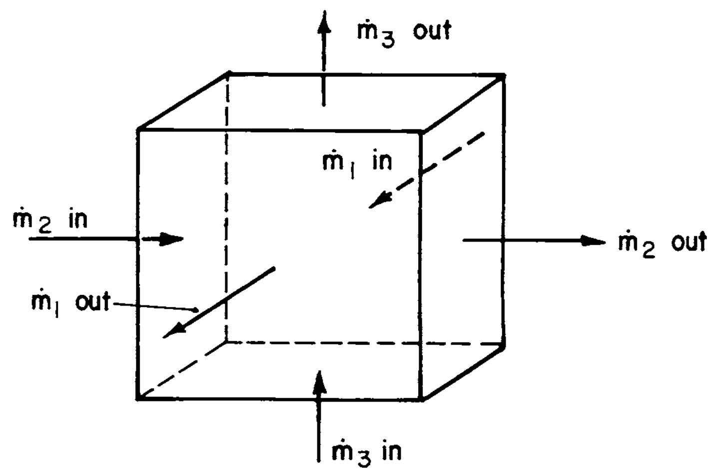

AIR FLOW RATE IN AND OUT

Fig. 4. Typical three-dimensional element showing velocity at centroid and air flow across element faces.

The bed model reported by Baird and Gaffney (1) required major revision for the current study. Each of the three-dimensional elements defined by the porous media flow analysis was treated like an individual bed similar to the bed model reported by Baird and Gaffney (1). However, a major difference between these two studies was the nature of the air flow. In the Baird and Gaffney (1) bed model, the air flow was one-dimensional or plug flow, while in the porous media flow analysis the air flow was three-dimensional. The three-dimensional nature of the air flow presented several analysis complications but the calculated velocity and pressure distributions allowed determination of the air flow rate at any location within the defined element model (orange carton).

A typical three-dimensional element is shown in Figure 4. The air flow rate in or out of each face of the element was determined from data provided by the flow model.

In order to determine the tmperature of the air entering a particular element from adjacent elements (or inlet boundary condition) the enthalpy entering each face of the element was used. The air entering through each face would mix within the element. Assuming ideal mixing and neglecting variation of the air density and specific heat, the resulting temperature from the mixture was calculated as illustrated below

(10) $\dot{m}_1 T_1 + \dot{m}_2 T_2 + \dot{m}_3 T_3 = \dot{m}_t T_m$

where

$\dot{m}_1, \dot{m}_2, \dot{m}_3$ = air flow rates entering element through faces 1, 2, and 3, respectively,

T_1, T_2, T_3 = temperature of air entering element through faces 1, 2, and 3 respectively,

$\dot{m}_t$ = total air flow rate entering element, $\dot{m}_1 + \dot{m}_2 + \dot{m}_3$

T_m = temperature as a result of perfect mixing.

Equation (10) was rearranged in terms of T_m to give

(11) $T_m = (\dot{m}_1 T_1 + \dot{m}_2 T_2 + \dot{m}_3 T_3) / \dot{m}_t$

T_m was the entering air temperature for the individual fruit model.

The "effective heat transfer coefficient", h, was obtained from Baird and Gaffney (1) who presented the following relationship:

(12) $h = 1.17\ (k_a/D)\ [\rho_a V_a D/\mu_a]$.

The velocity, V_a, in Equation 12 was defined as the superficial velocity. The best representative velocity for determining the convective coefficient from the model was identified as the calculated velocity at the centroid of the element. This velocity was defined as the superficial velocity by Ergun (5). The magnitude of the centroidal velocity vector, $|\bar{V}|$ was substituted for V_a in Equation 12 and provided the following relationship for determining the convective heat transfer coefficient in terms of the velocity at the centroid of the element:

(13) $h = 1.17\ (k_a/D)\ [\rho_a |\bar{V}|\ D/\mu_a]$.

Using the individual fruit model, the temperature at each point within the individual product for the specified time period and element was calculated.

The final step consisted of calculating the temperature of the air leaving the element. This was accomplished by an analysis similar to that used by Baird and Gaffney (1). The change in the energy of the air as it moved through the element (control volume) was equal to the change in the internal energy of the product within the element

$$\dot{m}_t\ c_a\ (\partial T_m/\partial v)\ dv\ dt = -\ \rho_p\ c_p\ (\partial T_p/\partial t)\ dt\ dv_p.$$

where

T_a, T_p = temperature of the air and product, respectively

A = cross-sectional area of the packed bed

ρ_a, ρ_p = density of air and bulk density of product, respectively

c_a, c_p = specific heat of air and specific heat of product, respectively

t = time

v, v_p = volume of the element and volume of the product, respectively.

The volume of the product is related to the volume of the element by the porosity, ϵ,

(14) $v_p = (1-\epsilon)v$

Inserting Equation 14 for the product volume in the energy balance above and solving for the change in air temperature resulted in the following:

(15) $\partial T_m/\partial v = -\ (1-\epsilon)\ [\rho_p\ c_p/\ \dot{m}_t\ c_a]\ \partial T_p/\partial t$.

By considering the differential control volume (element) to be a finite volume, Equation 15 was approximated by

(16) $\Delta T_m/\Delta v = -\ (1-\epsilon)\ [\rho_p\ c_p/\ \dot{m}_t\ c_a]\ \Delta T_p/\Delta t$.

The temperature leaving each face of an element was determined from the air temperature change calculated using Equation 16 and the value of the air temperature that entered the element calculated using Equation 11. Then the procedure was repeated for the next element. The flow diagram for a fourth Fortran program used to solve for the temperature response for the individual fruit model and Equation 16 is shown in Figure 5. The physical and thermal properties of size 100 Valencia oranges reported by Gaffney and Baird (6) were used for individual and modified bed models. For the vent locations used on the experimental carton, the flow model results were symmetric top and bottom. Therefore, only the bottom 700 elements were used in the heat transfer program in order to reduce the number of calculations required.

A Fortran program was written to reorganize the calculated temperature response so that the thermocouple locations in the model corresponded as closely as possible to the experimental thermocouple locations. The 78 thermocouple locations were assigned an air, product surface or center time dependent temperature value using the temperature value for a particular set of elements from the 700 elements available. The thermocouple location

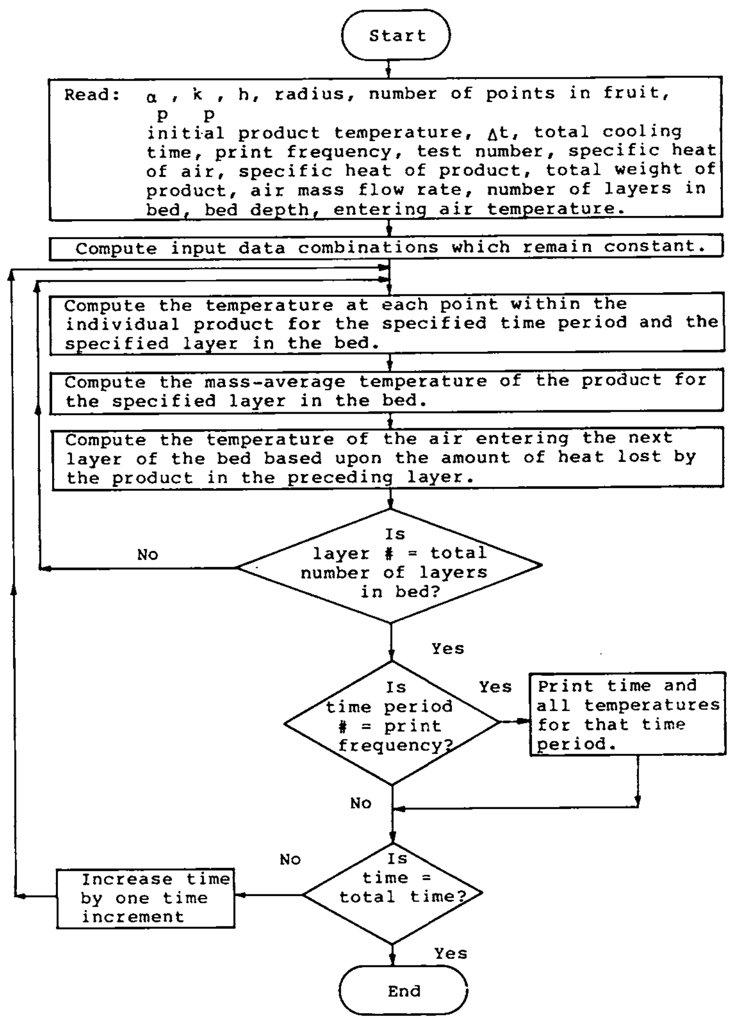

Fig. 5. Flow diagram for the computer program to solve orange carton heat transfer equations.

within the model was selected as close as possible to the physical location for the experimental carton.

Results and Discussion

From the twelve boundary conditions reported by Talbot (13), Boundary Condition 1-1 was selected for presentation. This boundary condition was one of the most difficult to model because of the low flow rate and restrictive single inlet and exit locations.

Six thermocouples from the first and third layers and 5 thermocouples from the second layer were selected for direct comparison of the temperature response curves of predicted versus experimental data. For each layer, 2 sets of 2 or 3 thermocouples were selected parallel to a line from inlet to exit. One set of thermocouples was located near the side of the carton and the other set was near the center of the center of the carton. For the left side of the third layer, thermocouples 31, 36, and 45, and 32, 39, and 46 were selected and plotted in Figure 6. For the left side of the second layer, thermocouples 23 and 26, and 24, 27, and 29, were selected and plotted in Figure 7. For the left side of the bottom layer, thermocouples 1, 10, and 15, and 4, 11, and 18, were selected and plotted in Figure 8.

In order to consolidate the large amount of data for each test into a more compact presentation, a regression plot of the predicted temperature versus the experimental temperature was formed for each thermocouple location

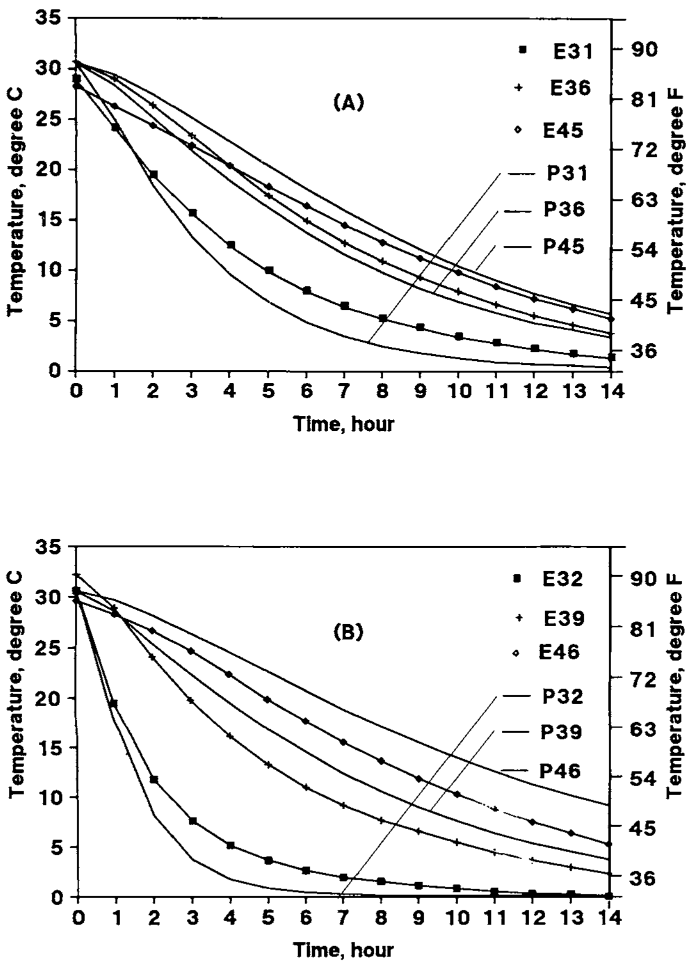

Fig. 6. Predicted versus experimental data for Boundary Condition 1-1, 3rd layer, thermocouples: (a) 31, 36, and 45; and (b) 32, 39, and 46.

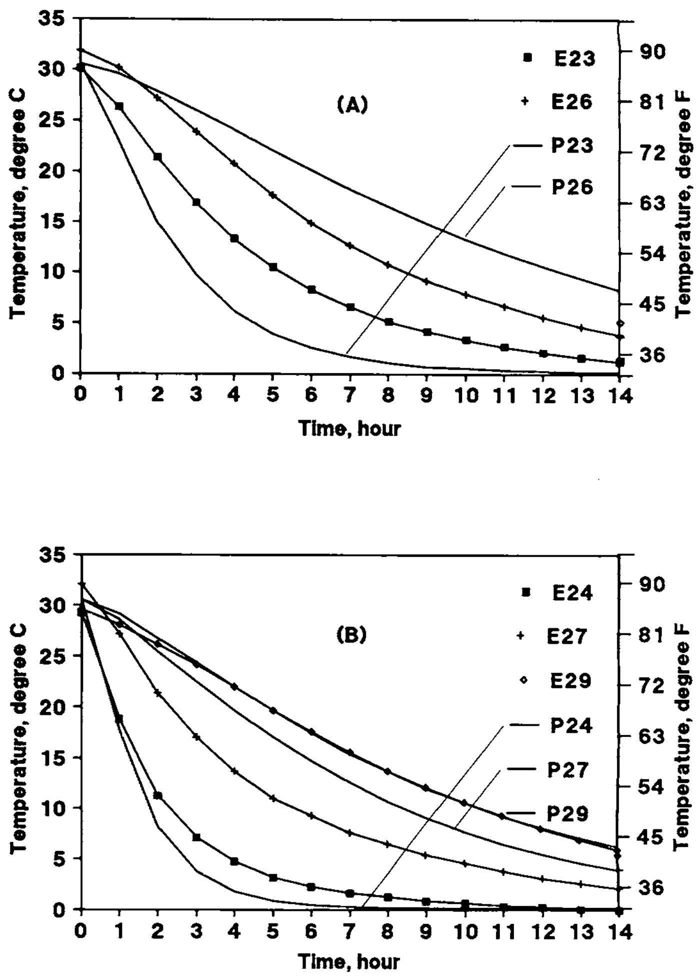

Fig. 7. Predicted versus experimental data for Boundary Condition 1-1, 2nd layer, thermocouples: (a) 23 and 26; and (b) 24, 27, and 29.

for the entire cooling test time. Center, surface, and air temperatures were all considered. For Boundary Condition 1-1 with a cooling test time of 14 hours, and Boundary Condition 3-2 with a cooling test time of 2.8 hours, the regression plots are presented in Figure 9.

Several trends exhibited by all 12 boundary conditions are evident in Figures 6 through Figure 8. The first trend indicated that the experimental and predicted cooling responses fit better for oranges near the walls of the orange carton (regions with increased porosity) than for oranges in the center or core of the orange carton. The oranges in regions with the least exposure to increased variable porosity exhibited a slower predicted versus experimental temperature response. This is opposite the trend reported by Talbot (13) and is attributed to the reduction of the central porosity with the increase in the variable porosity in the regions adjacent to the walls of the carton. In Figure 6a, for the corner thermocouple 31 and side thermocouple 36 in the left half of the third layer of oranges, the predicted data indicated more cooling than the experimental data. The same would have held for thermocouple 45 if not for the lower initial temperature of the exprimental data. In Figure 6b, the same trend applied for thermocouple 32 near the inlet vent, while the experimental data indicated a faster cooling rate than the predicted data for thermocouples 39 and 46. This illustrates a second general trend. The predicted cooling response for oranges near

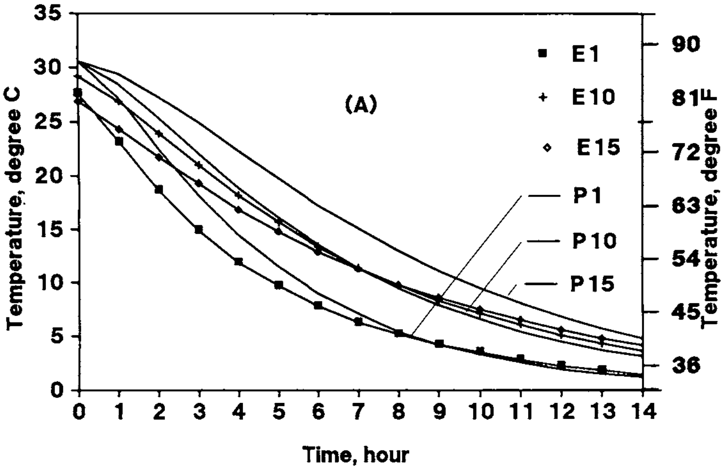

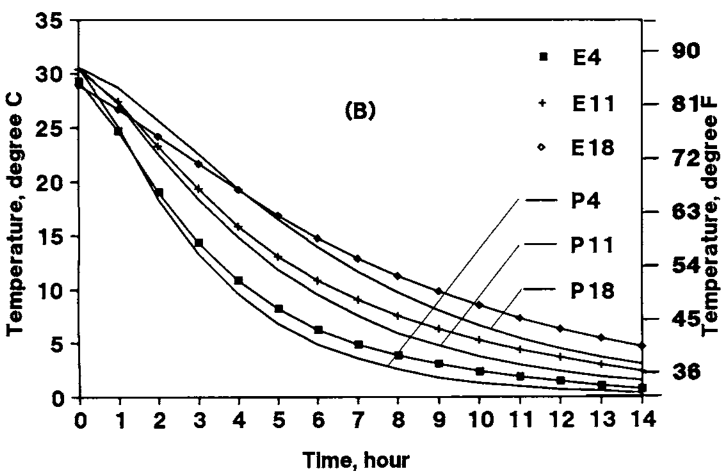

Fig. 8. Predicted versus experimental data for Boundfary Condition 1-1, 1st layer, thermocouples: (a) 1, 10, and 15; and (b) 4, 11, and 18.

the center of the cartons illustrated an increasingly poorer fit to the experimental temperature response as the distance from the air inlet increased. The difference between predicted and experimental temperature responses in the third layer for thermocouple 46 and thermocouple 32 illustrate this trend.

In Figure 7, the predicted response was lower than experimental data for thermocouples 23 and 24, which were in the second layer of oranges adjacent to the inlet carton. This was also a general trend. The predicted versus experimental data for second layer thermocouples 26 and 27 exhibited poor agreement. Thermocouple 26 was in the core of the orange carton near but not adjacent to the carton wall while thermocouple 27 was in the core of the orange carton, just below a line from the inlet to exit vent. Thermocouple 27 exhibited a better predicted to experimental data fit than thermocouple 26. Thermocouple 29 was adjacent to the outlet carton wall just below the outlet vent and the predicted and experimental data were in close agreement.

In Figure 7a, thermocouples 1, 10, and 15, are adjacent to the bottom near the side of the orange carton. As expected the predicted and experimental temperature responses indicate that the predicted temperatures would have cooled faster if not for the lower initial experimental temperatures. The predicted and experimental temperature responses of thermocouples 4, 11, and 18, in Figure 7b, also indicate a lower predicted than experimental temperature response.

In Figure 9, the regression plot of the predicted temperature versus the experimental temperature illustrates that the predicted data underestimated the cooling response of the oranges in the experimental carton. If the predicted and experimental data were identical, the data fitting line would have a slope of 1.0, while the actual data exhibited a slope of 0.93 and 0.96 for Boundary Condition 1-1 and 3-2, respectively.

Although the equipment and procedures used to measure the experimental temperature response have been developed and perfected over the last 10 years, there are a number of factors which directly effect the final temperature measurement. The instrumentation accuracy, the control of the air flow rate, the control of the inlet air temperature, the precise location of the thermocouples, the size and shape of the oranges, and the uniformity of packing the oranges, are but a few of the many variables which have a direct bearing on the final temperature readings. Considering these and other factors, the temperature readings are estimated to be within ± 2°F (1.1°C).

The initial temperature was obtained by reheating the carton of oranges as packed with thermocouples in place.

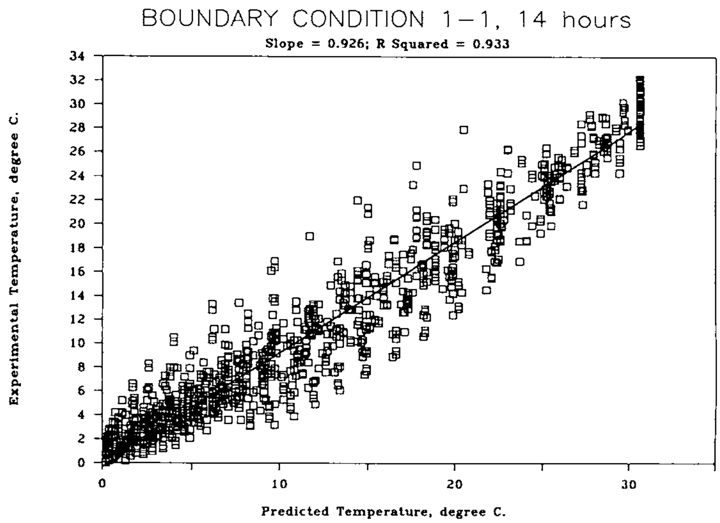

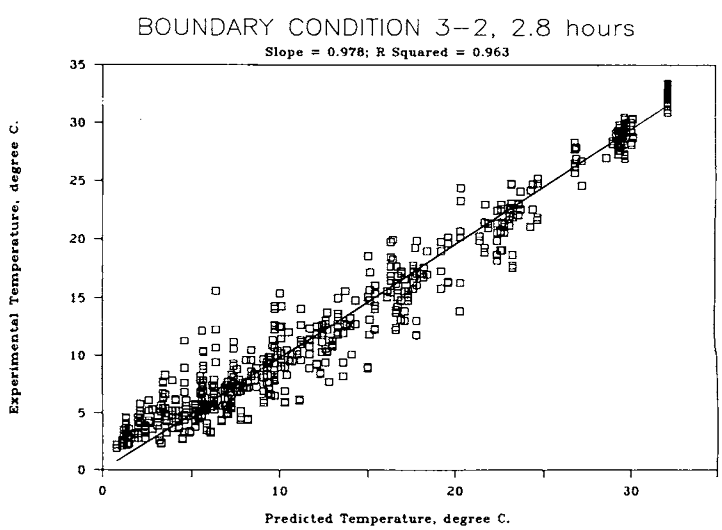

Fig. 9. Regression plot of the predicted temperature versus the experimental temperature for Boundary Conditions: (a) 1-1 and (b) 3-2.

Although it was possible to apply heat until the oranges were at almost the same steady state temperature, the amount of time required to accomplish this was excessive in terms of productivity as well as physiological maintenance of the oranges. Deteriorated oranges required the entire orange carton to be emptied and filled with a new load of oranges which had been prepared with thermocouples. The model required an initial product temperature and the average initial experimental temperature was used in the heat transfer model. The standard deviation was such that the experimental and model thermocouple initial temperatures could be slightly different up to 6°F (3.3°C). This altered the cooling curve of the model and produced a poorer comparison of experimental to model data (Figure 8a).

Over the several hours required for a complete test run, the air temperature control had a tendncy to drift if not manually corrected periodically. The model air temperature was a constant and did not account for actual test variations.

Because of a desire for increased accuracy 36-gauge thermocouple wire was used. However, this wire was very fine and easily damaged. Thermocouples were calibrated using an ice bath but at high temperatures slight variations between thermocouples were evident. Also the large number of thermocouple leads presented a requirement for diligent attention to detail.

The convective heat transfer coefficient reported by Baird and Gaffney (1) for cooling of oranges in beds was used in this study. This coefficient appeared to be satisfactory for the accomplishment of the current project objectives. In order to investigate the sensitivity of the model, one test was evaluated with the convective heat transfer coefficient halved and another with the coefficient doubled. The model was very sensitive to this forced change. Therefore if an improved value for the convective heat transfer coefficient were developed the model would provide a better fit of the experimental data.

A tendency in modeling research is to force the model to fit the experimental data. For this study a similar approach was not appropriate since the development and verification of a heat transfer model was not the objective. The major emphasis was the evaluation of the porous media technique for this type problem.

Preliminary evaluation of the model did not apply variable porosity and fit of the experimental data was very poor. A method for determining and applying the variable porosity was developed and this improved the fit of the predicted temperature response to that of the experimental temperature response.

Additional experimental work is needed to provide the necessary variable porosity data for various size and shape cartons, with various product packing arrangements. Increased porosity due to compaction near the top of the container should be also be addressed.

Future efforts should be made to design the element size and grid location to allow the physical location of the thermocouples to coincide with the center of a single element. This would provide a more reliable method for comparing experimental and numerical temperature response.

Summary

This study involved the application of several existing procedures in a unique way. A commercial finite element solution package was used to determine the pressure and velocity distribution for air flow through a porous media. This procedure first was verified by comparing the results from the porous media analysis with the results of research related to the pressure and velocity distributions for air flow through two- and three-dimensional grain bins. Based upon favorable results the porous media technique was used to model research concerning the pressure loss through oranges in bulk and oranges packed in simulated orange cartons. Again favorable results led to the evaluation of the pressure and velocity distributions of air flow through a three-dimensional orange carton using the finite element porous media flow analysis. However, the air flow field for the orange carton was not known and not readily measurable using current instrumentation. In order to verify the porous media analysis for this problem an indirect method of comparison was developed. The experimental temperature was measured for 12 different test conditions for oranges packed in an experimental orange carton and cooled using an experimental cooling facility. The flow and boundary conditions used for the twelve tests were used as input data for the porous media flow model to calculate the pressure and velocity distributions for the oranges packed in the experimental orange carton. The absolute permeability and the visco-inertial input parameters were calculated using experimentally determined Ergun product coefficients, orange diameter, and variable porosity. An existing heat transfer program was modified to incorporate the calculated velocity distribution and provided a predicted temperature response. Considerable work was involved after obtaining the calculated velocity distribution in order to determine the predicted temperature response. The experimental and predicted temperature responses for the 12 tests were compared and this comparison was used to indirectly evaluate the flow information calculated by the porous media flow analysis. Although several areas for improvement were noted the porous media flow analysis was found to provide valuable information if variable porosity within the orange carton was considered. The objective of this study was not to develop a comprehensive model to evaluate the many variables related to forced air cooling and to predict the cooling response of produce packed in containers. However, the porous media flow model and heat transfer model have the capability to solve the pressure and velocity distributions and temperature response for any size and shape carton, any size, number and location of vent holes, any packing arrangement, any size (close to spherical) fruit or vegetable, for any air flow rate and cooling temperature typically encountered in the field. Suggested improvements will produce a very valuable tool for designing systems for cooling fruits and vegetables in cartons.

Literature Cited

1. Baird, C. D. and J. J. Gaffney. 1976. A numerical procedure for calculating heat transfer in bulk loads of fruits and vegetables. ASHRAE Transactions 82(2):525-540.
2. Baird, C. D, J. J. Gaffney, and D. T. Kinard. 1975. Research facility for forced-air precooling of fruits and vegetables. Transactions ASAE 18(2):376-379.
3. Chau, K. V., J. J. Gaffney, C. D. Baird, and G. A. Church III. 1983. Resistance to air flow of oranges in bulk and in cartons. ASAE Paper 83-6007.
4. DeSalvo, G. J. and J. A. Swanson. 1983. ANSYS engineering analysis system user's manual. Swanson Analysis Systems, Inc. Houston, PA.

5. Ergun, S. 1952. Fluid flow through packed columns. Chem. Eng. Progress 48:89-94.
6. Gaffney, J. J. and C. D. Baird. 1980. Physical and thermal properties of Florida Valencia oranges and Marsh grapefruit as related to heat transfer. ASAE Paper 80-6011.
7. Guillou, R. 1960. Coolers for fruits and vegetables. Calif. Agr. Expt. Sta. Bul. 773. 66 p.
8. Khompis, V., L. J. Segerlind, and R. C. Brook. 1984. Pressure patterns in cylindrical grain storages. ASAE Paper 84-3011.
9. Pillai, K. K. 1977. Voidage variation at the wall of a packed bed of spheres. Chem. Eng. Sci. 32:59-61.
10. Ridgway, K. and K. J. Tarbuck. 1968. Voidage fluctuations in randomly-packed beds of spheres adjacent to a containing wall. Chem. Eng. Sci. 23:1147-1155.
11. Segerlind, L. J. 1982. Solving the nonlinear airflow equation. ASAE Paper 82-3017.
12. Stanke, V. and E. Eckert. 1979. A study of the area porosity profiles in a bed of equal-diameter spheres confined by a plane. Chem. Eng. Sci. 34:933-940.
13. Talbot, M. T. 1987. Pressure and velocity distribution for air flow through fruits packed in shipping containers using porous media flow analysis. Ph.D. Dissertation, University of Florida. University Microfilms, An Arbor, Michigan.

Proc. Fla. State Hort. Soc. 101:175-182. 1988.

EVALUATING PRECOOLING METHODS FOR VEGETABLE PACKINGHOUSE OPERATIONS

STEVEN A. SARGENT[1], MICHAEL T. TALBOT[2], AND JEFFREY K. BRECHT[1]
Vegetable Crops Department[1]
Agricultural Engineering Department[2]
University of Florida, IFAS
Gainesville, FL 32611

Additional index words. systems analysis, precooling schedule.

Abstract. **Temperature management is essential in maintaining vegetable quality during postharvest handling operations. For many crops, precooling is the recommended procedure to extend storage life sufficiently for shipping and retailing. The objectives of this paper are: 1) to provide information concerning recommended storage conditions for selected vegetable crops; 2) to provide a procedure for evaluating harvest and handling operations for addition or modification of precooling systems; 3) to explain precooling principles and methods; and 4) to present a simple, yet accurate method for determining precooling schedules as part of an overall quality control program in the packinghouse.**

The value of 1986-87 Florida vegetable crops exceeded $1 billion; of the total production for this growing season, 75% was shipped to other states, and exported to Canada and other countries (1).

The key to maintaining present markets and securing new markets lies in the ability of shippers to consistently supply high quality produce capable of withstanding subsequent handling to distant markets. *Quality* refers to those characteristics which consumers associate with each commodity that are dependent upon the particular end-use, such as sweetness in melons and sweet corn, tenderness in snapbeans, and crispness in carrots and cucumbers. It also refers to freedom from bruises, blemishes, disorders, diseases and shrivel.

Precooling is the rapid removal of field heat to temperatures approaching proper storage temperature and is the first line of defense in slowing the biological processes which reduce product quality. It has been in use in Florida since the introduction of hydrocooling of celery in the 1920's (9). Precooling, in conjunction with refrigeration during subsequent handling operations, provides a cold chain to maximize storage life and control disease and pests. The term "storage life" is purposely used in this text, since "shelf life" has the connotation that the commodity "sits on the shelf", implying no subsequent refrigeration.

The keyword to produce quality maintenance is "timeliness"; timely and careful harvest and transport to the packinghouse, rapid packing and precooling, and rapid transport to the market or buyer. Also, once a product is cooled, the cold chain must not be broken during subsequent handling.

Although many larger packinghouses incorporate precooling in their handling operations, smaller packinghouses often rely on short-term storage in refrigerated rooms or in some circumstances load directly into refrigerated trailers. Refrigerated trailers, in particular, should not be loaded with produce which has not been adequately precooled since most trailers are designed to maintain temperature and as such *do not* have the additional refrigeration capacity necessary to remove field heat from an entire load of produce.

There are many excellent publications available which provide great detail concerning individual precooling methods. A selected group for further study includes: Hardenburg, et al. (3), Kader, et al. (4), Mitchell. et al. (6), Ryall and Lipton (7), and Stewart and Couey (10). The purpose of this report is to systematically review the chief concerns which must be addressed when evaluating a particular packinghouse operation for precooling. These concerns include:

1) storage requirements for various crops;
2) evaluating harvest and handling operations;
3) precooling concepts and methods;
4) determining precooling schedules.

1. *Storage requirements*

The storage life or relative perishability of a crop is reflected in its respiration rate. Once harvested, a vegetable continues life processes independent of the plant, and as a result, must utilize its own reserves. Many crops, such as greens, celery and lettuce, are cut at harvest which causes additional stress. Respiration is the process of life by which oxygen is combined with stored carbohydrates and other components to produce heat, chemical energy, water, carbon dioxide and other products. The respiration rate varies by commodity; those commodities with a high respiration rate utilize the reserves faster and are more

Florida Agricultural Experiment Station Journal Series No. 9704. The authors wish to thank Judy Zoellner, Vegetable Crops Dept., for preparation of the graphic materials.